Conditioned Medium of Mesenchymal Stem Cells Decreases Liver Fibrosis Caused by Acetaminophen by Suppressing the Systemic Inflammatory Response.

Andrey Temnov (andtemnov@gmail.com)
Moscow Institute of Physics and Technology
Alla Sklifas
Institute of Cell Biophysics
Vitaly Zhalimov
Institute of Cell Biophysics
Mars Sharapov
Institute of Cell Biophysics
Alexey Kodunov
Intersectoral Research and Technology Complex Eye Microsurgery
Konstantin Rogov
RESEARCH INSTITUTE OF HUMAN MORPHOLOGY

Research Article

Keywords: Acetaminophen, liver, fibrosis, stem cells, conditioned media

Posted Date: April 26th, 2021

DOI: https://doi.org/10.21203/rs.3.rs-418373/v1

CONDITIONED MEDIUM OF MESENCHYMAL STEM CELLS DECREASES LIVER FIBROSIS CAUSED BY ACETAMINOPHEN BY SUPPRESSING THE SYSTEMIC INFLAMMATORY RESPONSE.

A.A.Temnov[1], A.N.Sklifas[2], V.K.Zhalimov[2], M.G.Sharapov[2], A.M.Kodunov[3], K.A.Rogov[4]

Moscow Institute of Physics and Technology (MIPT), Dolgoprudny, Moscow Region,
Institute of Cell Biophysics of the Russian Academy of Sciences, PSCBR RAS, Pushchino, Moscow Region, Russia
S. Fyodorov Eye Microsurgery Federal State Institution, Russia
Research Institute of Human Morphology, Moscow, Russia

Corresponding author: A.A.Temnov andtemnov@gmail.com

Abstract

This study explored the effect of mesenchymal stem cells (MSC) conditioned medium (CM) on the severity of systemic inflammatory response caused by acetaminophen administration. The long-term effects of the toxin on the liver tissue were analysed. The effect of a fraction of the conditioned medium on the functional activity of isolated neutrophils was investigated using a model of sterile inflammation. The study showed that the >30 kDa CM fraction possesses the maximum protective effect. Proteins of this fraction reduce the severity of the systemic inflammatory reaction and the extent of liver tissue fibrosis after the toxin injection in the long term. By using the sterile inflammation model, CM was shown to reduce the complex activity of NADPH oxidase, which leads to a decrease in the total reactive oxygen species production. The CM derived from the cultivation of stem cells reduces the severity of the systemic inflammatory response through suppression of the functional activity of neutrophils.

Key words: Acetaminophen, liver, fibrosis, stem cells, conditioned media

INTRODUCTION

Acetaminophen (APAP) overdose, especially attended by the depletion of the glutathione detoxification system, leads to severe damage of the liver parenchyma and development of acute liver failure, which can result in the death of a patient (Larson AM 2007; McGill MR, Jaeschke H. 2013; McGill MR et al. 2012).

N-acetyl-para-benzoquinone is an active metabolite of APAP. It binds to cellular proteins, damaging hepatocyte mitochondria and mitochondrial DNA and causing hepatic death (McGill MR et al. 2012). Massive hepatic necrosis and release of intracellular proteins from hepatocytes into the bloodstream cause activation and migration of granulocytes and their subsequent penetration into the liver parenchyma (Jaeschke H et al. 2012). The amount of further damage to hepatocytes caused by this process is being debated. Several researchers believe that hyperactivated neutrophils increase the extent of liver damage (Ishida Y et al. 2006; Liu ZX et al. 2006; Marques PE et al. 2012). Others argue that there is no direct evidence of cellular damage associated with neutrophil function (Cover C et al. 2006; Hou HS et al. 2012; Lawson JA et al. 2000; Williams CD et al. 2010a; Williams CD et al. 2010b; Williams CD et al. 2014).

Nevertheless, the very fact of neutrophil migration into the liver tissue under the toxic effect of APAP is conclusive (Jaeschke H et al. 2012).

In vitro, APAP is a potent quencher of reactive metabolites such as HOCl and hydrogen peroxide (released by neutrophils), which is a possible reason, explaining the difficulty to assess the role of granulocytes in APAP-induced liver damage (Freitas M et al. 2013). A decrease in APAP concentration in tissues during the process of detoxification possibly leads to an increase in the concentration of reactive oxygen species (ROS) formed by neutrophils. This development is likely to enhance liver damage in the later stages of the pathological process.

In our opinion, the crucial role belongs to the NADPH oxidase complex, which is responsible for the production of ROS in various cells and tissues. Several studies have shown that NADPH oxidase activity is increased with APAP in hepatocytes, and NADPH oxidase inhibition significantly reduces the severity of hepatocellular damage (Wang JX et al. 2017).

At the same time, we cannot exclude that a decrease in NADPH oxidase activity in granulocytes can also suppress ROS production and lessen the liver parenchyma damage.

In our previous studies, we have demonstrated that the conditioned medium (CM) obtained from the cultivation of mesenchymal stem cells (MSCs), especially the >30 kDa fraction, exerts a protective effect during APAP-induced acute liver failure (Temnov AA et al. 2019; Temnov A et al. 2019). We registered a decrease in the extent of granulocytic infiltration around the portal veins as one of the main pathological features.

The aim of the present study was to assess the level of granulocytic infiltration and longterm results under the toxic effect of APAP, as well as to estimate the impact of conditioned medium derived from stem cell cultivation (>30 kDa) on the production of ROS by the NADPH oxidase complex in neutrophils using the sterile inflammation model.

MATERIALS AND METHODS

Modeling acute liver failure.

The study protocol was approved by the institutional Ethics Committee of the Institute of Cell Biophysics RAS (PSCBR RAS) and was in compliance with ARRIVE guidelines. All methods were also performed in accordance with the relevant guidelines and regulations. All the experiments were carried out according to international regulations listed in the European Convention for the Protection of Vertebrate Animals used for Experimental and Other Scientific Purposes (ETS 123) and ICB RAS. Manual for Working with Laboratory Animal no. 57 (30.12.2011).

Male CD1 line mice weighing 22-24 g were divided into four groups. Animals in all the groups were intraperitoneally injected with 270 mg/kg APAP. Mice in the control group (No. 1, n=15) were intraperitoneally injected with 0.5 ml of culture medium (DMEM medium with fetal bovine serum, protein concentration 0.5 mg/ml). The animals in the first treatment group (No. 2, n=15) were injected with 0.5 ml of conditioned medium obtained from the cultivation of mouse MSCs (total fraction, protein concentration 0.5 mg/ml). Animals in the second

treatment group (No. 3 n=15) were injected with the >30 kDa fraction of conditioned medium obtained from the cultivation of MSCs (protein concentration 0.5 mg/ml). Animals in the third treatment group (No. 4, n=15) were injected with 0.5 ml of MSC suspension (10^6 cells/ml).

Bone marrow stem cell isolation. To isolate MSCs, bone marrow was obtained from the femur of CD1 mice under Zoletil™ general anesthesia. The mononuclear fraction of bone marrow cells was isolated on a density gradient using a standard Lympholyte-H solution (Cedarlane, Canada) following a set methodology. A suspension of mononuclear cells was plated on Petri dishes and cultured in DMEM medium supplemented with 10% fetal bovine serum (Gibco) in a CO_2-incubator with the atmosphere composition of 10% O_2, 5% CO_2 and 85% N_2.

Osteogenic, chondrogenic and adipogenic cellular differentiations were conducted with growth factors following a standard methodology in order to confirm that the cells have MSCs properties (Yagi H et al. 2010).

The analysis of MSCs phenotypic profile showed the presence of the following markers: CD73+ in 98.7% of cells, CD44+ in 98.0%, CD105+ in 94.6%, CD34+ in 0.1%, CD45+ in 0.3%.

Obtaining MSC conditioned medium. The cultured medium was completely replaced after obtaining a cell monolayer, and three days later, the conditioned medium was combined with MSC lysate.

Obtaining the fraction of conditioned medium. Ultrafiltration with Minimate TFF Capsule Omega 30K filter (Pall, USA) was used to separate the conditioned medium. A fraction primarily containing proteins weighing >30 kDa was obtained.

Histology. Material for histological examination was collected 4, 24 and 96 hours after the administration of APAP. Samples of animal tissue were collected on day 10 to assess the longterm effects of APAP. Mice liver specimens were fixed in the 10% neutral buffered formalin for morphological assessment of changes.

Pathomorphological changes in the liver tissue were assessed on a 0 to 3 point scale (0 - no change; 1 - more than 1/3 of the area was changed; 2 - more than 2/3 of the area was changed; 3 - 100% of the area was changed). Biopsies from 6 animals were studied for scoring in each group.

Biochemical study. The level of the hepatic enzyme GOT (aspartate aminotransferase) was measured in whole blood using a Reflatron biochemical analyzer (Roche, USA) before the start of the experiment, as well as 4, 24, 48, and 96 hours after APAP administration.

Gene expression assessment mRNA isolation.

Total RNA was extracted from 4–6 mg liver using ExtractRNA reagent (Evrogen, Russia) following the manufacturer's protocol. RNA quality was assessed by the presence of 18S and 28S rRNAs using electrophoresis in 2% agarose gel. RNA concentration was determined using a NanoDrop 1000c spectrophotometer (USA).

Conducting qPCR with reverse transcription (RT-qPCR).

Two micrograms of total RNA was used per reverse transcription reaction with MMLV reverse transcriptase and standard dT_{15} oligonucleotide (Evrogen, Russia) following the manufacturer's protocol.

The obtained cDNA was used for real-time PCR with gene-specific primers (Table 1) and qPCRmix-HS SYBR kit (Evrogen, Russia). Real-time PCR was carried out using DNA amplifier CFX96 (Bio-Rad, USA). The PCR cycling regime was as follows: (1) "hot-start" 95 °C, 5 min; (2) denaturation 95 °C, 15 s; and (3) primer annealing and DNA synthesis at 60°C, 30 s. Stages (2) and (3) were repeated 40 times. The threshold cycle (Ct) value was determined using Bio-Rad software. The gene expression data were normalized to the housekeeping gene of cytoskeletal betaactin (Actb). The change in gene expression was calculated using the 2-ΔΔCt method (Schmittgen TD, Livak KJ. 2008).

Table 1. Oligonucleotides used for qRT-PCR.

Genes	GenBank #	5'-3'	Amplicon size (bp)
Actb	NM_007393.4	F: AGCCATGTACGTAGCCATC	149
		R: CTCTCAGCTGTGGTGGTGA	
Ki67	NM_001081117	F: ATCATTGACCGCTCCTTTAGGT	104
		R: GCTCGCCTTGATGGTTCCT	
Caspase 3	NM_009810	F: AAGGAGCAGCTTTGTGTGTG	145
		R: GAAGAGTTTCGGCTTTCCAG	
IL6	NM_031168	F: TAGTCCTTCCTACCCCAATTTCC	76
		R: TTGGTCCTTAGCCACTCCTTC	
THIO	NM_011660.3	F: GTGGTGGACTTCTCTGCTAC	94
		R: GGAACACCACATTGGAATAC	
Mif	NM_010798.3	F: GTGGTGGACTTTGCCAGAGG	95
		R: CACGTGCACTGCGATGTACC	
LEG1	NM_008495.2	F: GAACACCGGGAACCTGCCTT	94
		R: CTGGCAGCTTGATGGTCAGG	

Preparation of peritoneal neutrophils

Inflammation of three strains in mice was induced by intraperitoneal injection of zymosan suspension (5 mg/ml, 150 µl per mouse). Five hours later, the peritoneal cavity was washed with 3 ml Ca^{2+}-free Hanks' balanced salt solution (HBSS, pH 7.4, 4°C), wash-out was centrifuged for 5 min (600 g at 4°C). The purity of polymorphonuclear neutrophils (PMN) population exceeded 95%, as estimated by luminescent microscopy (LeicaDM6500, ×40) with acridine orange staining. The survival rate of cells was 97–99%, as determined by trypan blue staining. Isolated cells were kept in HBSS without Ca^{2+} and phenol red for 1 h at 4°C before use.

Chemiluminescence analysis

The intensity of reactive oxygen species (ROS) generation was estimated by luminoldependent chemiluminescence using a CHEMILUM-12 device (Institute of Cell Biophysics of the Russian Academy of Sciences, Pushchino, Russia) (Tikhonova IV et al. 2018). The experiment design was as follows: peripheral blood collected to Sarstedt tubes with heparin (Germany) was diluted with Ca^{2+}-free Hanks' solution (1:1) and kept for 1 h at 4°C. Specimens for measurements were prepared in polypropylene mini-dishes, which contained 173 µl Hanks' solution with 1 mM Ca^{2+}; 7 µl luminol (0.35 mM) and 20 µl diluted blood. After recording a spontaneous level of ROS, blood samples were activated with serum-opsonized

zymosan (0.25 mg/ml).Respiratory burst in isolated cells was initiated with 5 □M N-N-formyl-Met-Leu-Phe (fMLF). In brief, each independent experiment included 12 mini-dishes with samples (200 µl; 10^6 cells/ml). Samples of cells, prepared in a duplet, were: (i) PMN of the control and (ii) PMN of the experimental animals. 100 µM concentration of NaN_3 and 1 U/ml of horseradish peroxidase were used to inhibit myeloperoxidase (Foyouzi-Youssefi R et al. 1997).

After detecting the base level of chemiluminescence intensity, fMLF at a concentration of 5 µM was added to initiate the respiratory burst. The recording was done consecutively for all mini dishes for 2.5 s and continued for 10–30 min. Total ROS production was calculated as the area under the curve of chemiluminescence intensity in time. The effect of CM was calculated as the ratio of the cell parameters of treated animals to that of the control animals' cells. Each independent experiment was done with the cells of an individual animal.

Statistical analysis of collected data was conducted with Statistica 6.0 software. For nonparametric data, the Mann-Whitney U test was used. Differences were considered statistically significant at $p < 0.05$.

RESULTS

Biochemical study

The first stage of the analysis assessed the modes of administration of the conditioned medium into the animal body. The efficiency of the method was determined by the levels of the cytolytic GOT enzyme in the blood, which is released from damaged hepatocytes under the toxic effect of APAP products (Fig. 1).

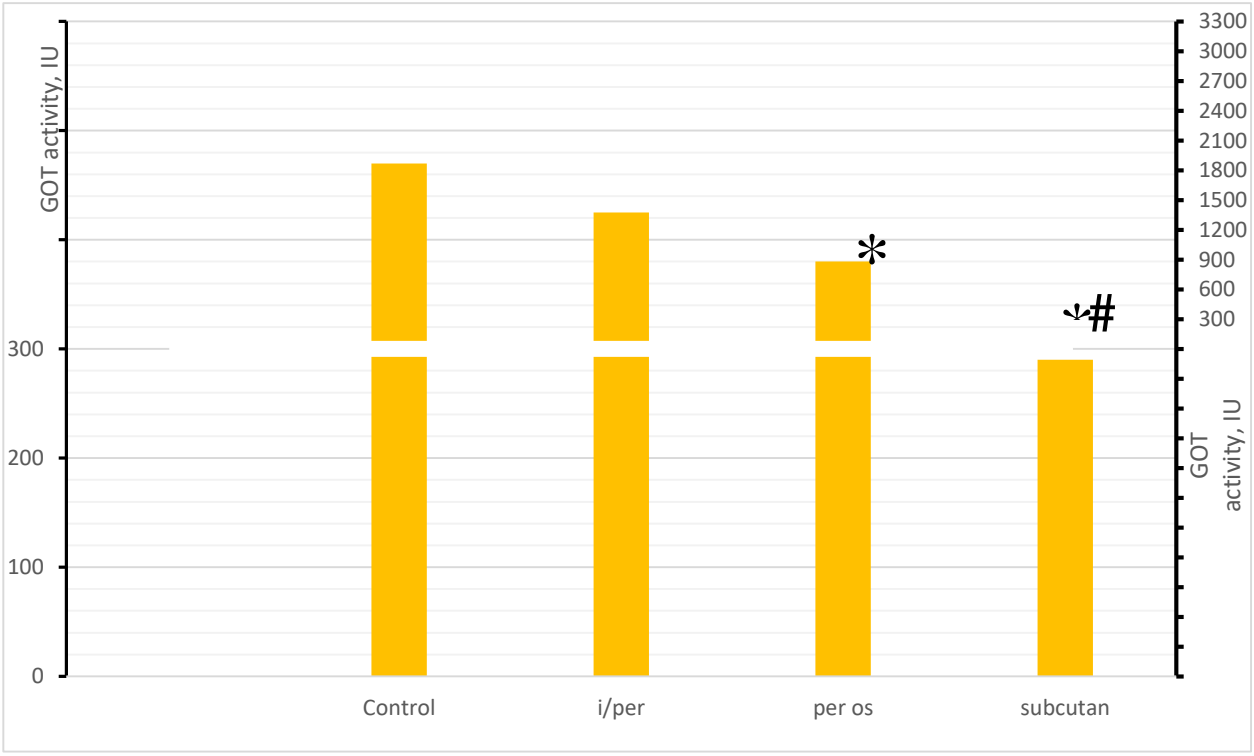

Figure 1. Activities of liver enzyme GOT (n=15 for each group) in the control group and in animals treated with CM hours after administration of APAP. *- true for the control group ($p<0.05$); #- true for other groups ($p<0.05$).

As shown in Figure 1, intraperitoneal injection appeared to be the least effective method, as testified four hours after the onset of APAP: the cytolytic enzyme level decreased by 19% from control. Oral administration and subcutaneous injection demonstrated a decrease of 46% and 75%, respectively. Thus, subcutaneous route of APAP administration in the subsequent experiments.

The next stage of the analysis examined a sharp increase in the level of cytolytic enzyme observed 4 hours after intraperitoneal administration of MSCs under the effect of APAP (Fig. 2; 28% increase compared to the control group variable). Notably, this increase in the level of cytolytic enzyme in the blood compared to the control was recorded during the first two days after the administration of MSCs. A sharp increase in hepatocyte proliferation was observed 24 hours after MSC transplantation. This process can lead to enhanced cell sensitivity to toxins and proinflammatory cytokines. By day 4, the level of the enzyme decreased and became the lowest among the groups.

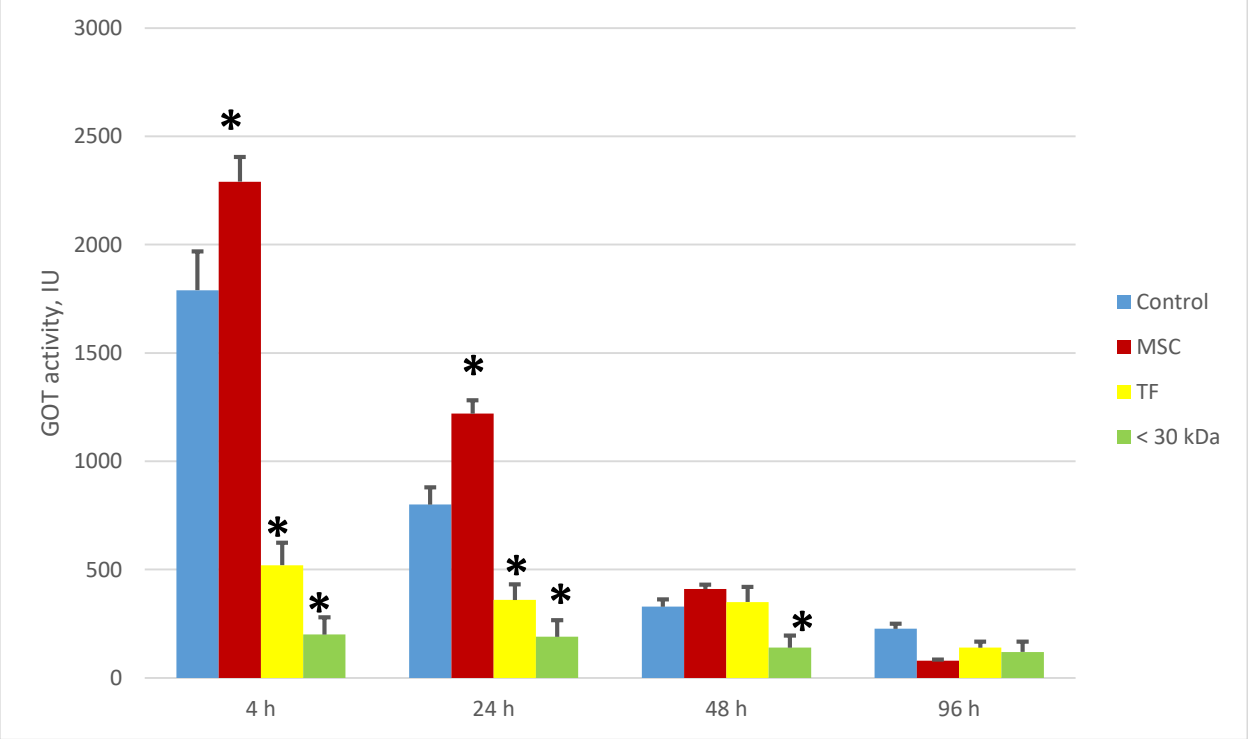

Figure 2. Changes in the activity of GOT under the influence of MSCs and CM in the blood under administration of APAP. *- true for the control group ($p<0.05$).

Subcutaneous injection of the total fraction (TF) of the conditioned medium caused a significant 75% decrease in the cytolytic enzyme level in the first 4 hours and a 50% decrease during the first 24 hours (compared to the control).

Subcutaneous injection of the >30 kDa fraction led to a maximum significant decrease in the level of GOT in the blood at the beginning of the acute stage after APAP administration (85% of the control).

Gene expression

The process of hepatocyte proliferation, triggered by severe damage, could be one of the possible reasons for the intensification of liver parenchyma necrosis in the acute damage stage upon administration of MSC. In this regard, we studied the changes in the expression (mRNA level) of Ki-67 (which is a marker of proliferative activity) in liver tissues under the effect of transplantation of MSC and conditioned medium.

Figure 3 shows that administration of CM (both the total fraction and >30 kDa fraction), obtained through MSC cultivation, caused a sharp decrease in Ki-67 expression during the first two days. Later (on day 4), the expression level of Ki-67 increased twice over the control.

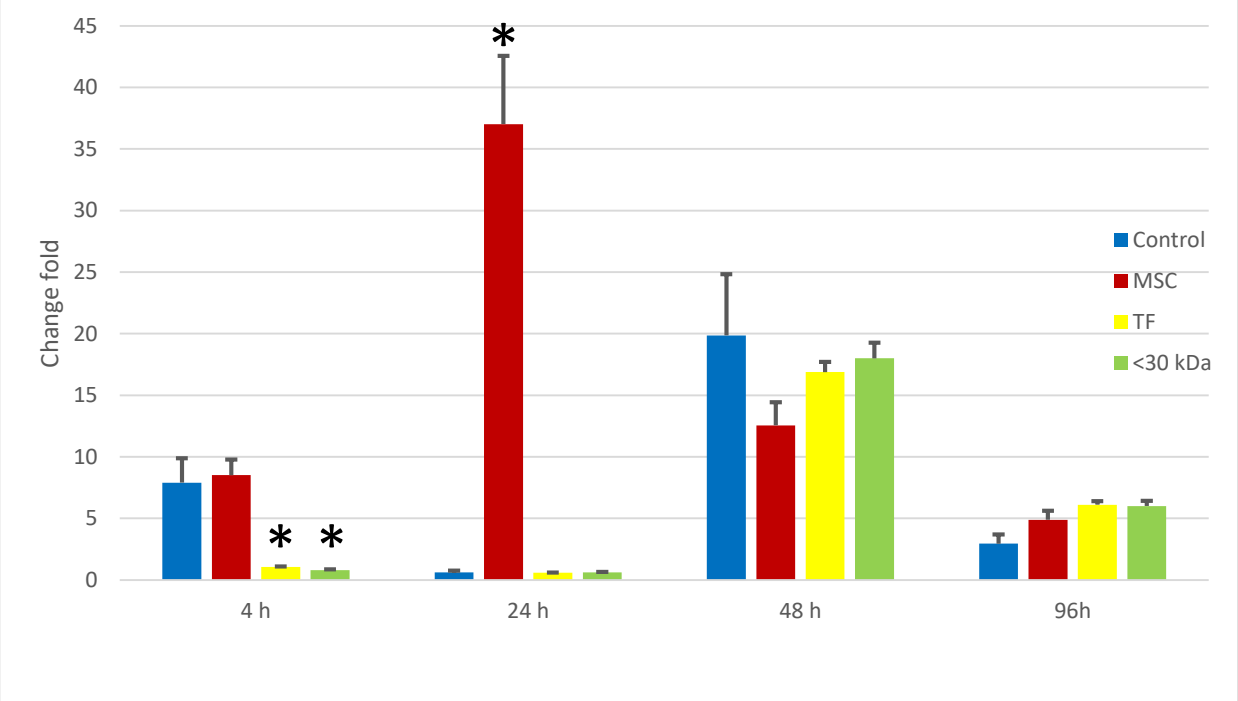

Figure 3. Changes in the expression of the Ki-67 gene (mRNA level) under the influence of MSCs and CM in the liver tissue. Data normalized to beta-actin . *- true for the control group ($p<0.05$).

Table 2. Change in the level of gene expression when >30 kDa fraction of the CM is used in the presence of APAP.

Gene name	Multiplicity of expression level relative to control			
	4 hours	24 hours	2 days	4 days
Mif2	1,3	3,2*	1,1	0,9
LEG1	1,1	1,4	0,6	1,4
Caspase	1,1	1,4	0,8	1,1
Il6	0,6*	0,3*	0,8	0,8
THIO	1,4	1,7*	1,3	0,6

*- true for the control group ($p<0,05$).

The analysis of gene expression revealed that under the effect of >30 kDa CM there is a change in the activity of genes that have both pro-inflammatory and anti-inflammatory effects. As shown in Table 2 data, CM induces a significant increase in the expression of thioredoxin synthesis gene. Enhanced expression of this enzyme 24 hours after the administration of the conditioned medium under APAP concurs with a decrease in the expression of IL-6, which has proinflammatory activity.

Histology

Analysis of histological sections revealed a maximum level damage of the liver parenchyma after 4 hours both in the control group and in the group treated with MSCs (Fig. 4).

Animal tissues from the control group exhibited portal vein fluid overload and fusion of extensive plethoric centrilobular regions of the hepatic lobules. The area of hepatic necrosis ranged from 35 to 50%. With MSC administration, the plethoric condition of portal veins was preserved similarly to the control group. The damaged area in the centrilobular region was decreased by 510% to the control. When the total fraction was used, the plethora area around the portal veins significantly reduced compared to the control and the MSC group. Upon use of the >30 kDa fraction, the fluid overload of the portal veins was undefined. Regions of centrilobular fluid overload were minimal when compared to the total fraction.

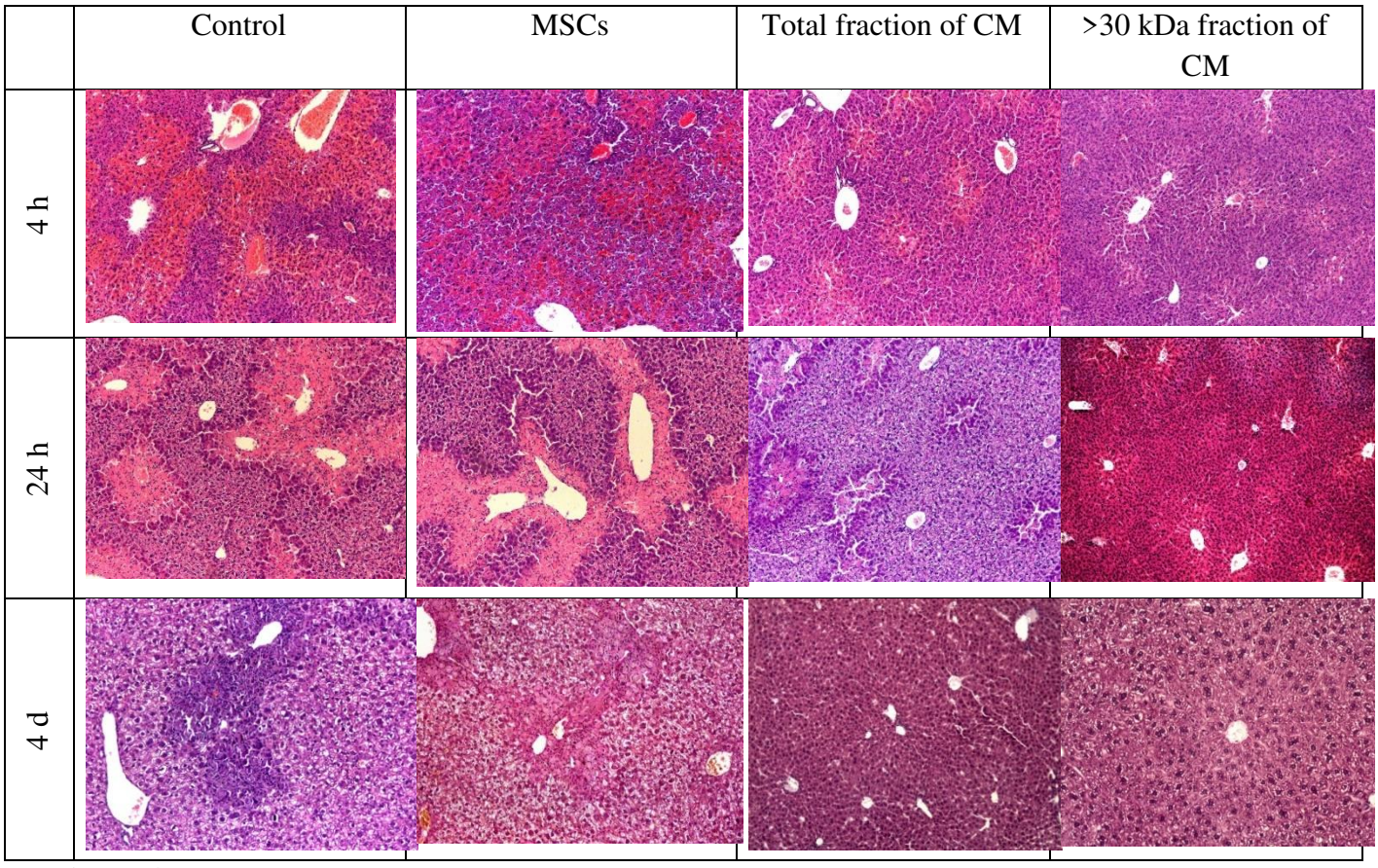

Figure 4. The effect of MSCs and CM on liver histology in the presence of APAP

Therefore, 4 hours after APAP exposure, a significant decrease in the damaged area was observed after administering the TF of the CM derived from MSC cultivation (figure 4). A

minimal toxic effect was registered when the >30 kDa fraction was used. 24 hours after APAP exposure, histological data analysis showed the following:

- extensive, merging areas of hepatocyte necrosis in centrilobular regions in the control group. A narrow strip of regenerating hepatocytes (characterized by more intense staining of the cell cytoplasm) was noted in the areas adjacent to necrosis.
- in the group treated with MSCs, extensive areas of centrilobular necrosis remained as well. Proliferation of hepatocytes was observed along the boundary of necrotic areas. In the group treated with the whole fraction of the conditioned medium, centrilobular necrosis sites were minimal in size, forming separate lobules. When the >30 kDa protein fraction was used for 24 hours, no necrosis was detected in the centrilobular regions of the hepatic lobules. However, these areas exhibited a moderate plethora (fluid overload).

On day 4, analysis of histological materials revealed that centrilobular necrosis areas were replaced by an extensive inflammatory infiltrate in the control group. Degenerative changes in hepatocytes were observed in the other hepatic lobules (200x magnification). In the MSC transplantation group, the severity of inflammatory infiltration was significantly lower than in the control group. However, similarly to the control, the degeneration of hepatocytes persisted across the rest of the lobules (200x magnification).

Unlike the previous two groups, the animals treated with the total CM fraction had no inflammatory infiltrates across the entire area of hepatic lobules, including the centrilobular region. No necrotic changes were found in the centrilobular region when using the >30 kDa fraction, either. Multiple regenerating hepatocytes were observed as well (200x magnification).

Table 3. The analysis of morphological changes in liver tissue during MSC transplantation and the use of CM in the presence of APAP. (0 - no change; 1 - more than 1/3 of the area was changed; 2 - more than 2/3 of the area was changed; 3 - 100% of the area was changed)

Timeframe	Variable	Control	MSC	fraction	>30 kDa
4 h	Portal vein fluid overload (plethora)	+++	+++	++	-
	Centrilobular regions fluid overload	+++	+++	++	+
	Hepatocyte degeneration	+++	++	+	+
24 h	Hepatocyte degeneration	+++	++	+	+
	Centrilobular necroses	+++	++	+	-
	Hepatocyte regeneration	+	++	++	+++
4 d	Inflammatory infiltrates	+++	+	-	-
	Hepatocyte degeneration	+++	++	+	+
	Hepatocyte regeneration	-	-	++	+++

The morphometric analysis implemented for comparison of the identified changes showed that the use of the >30 kDa fraction of conditioned medium reduces the level of hepatocyte damage and the severity of the inflammatory reaction and promotes earlier initiation of regeneration processes (Table 3). The long-term effect of MSCs and the conditioned medium on the growth of connective tissue under the toxic effect of APAP was studied separately.

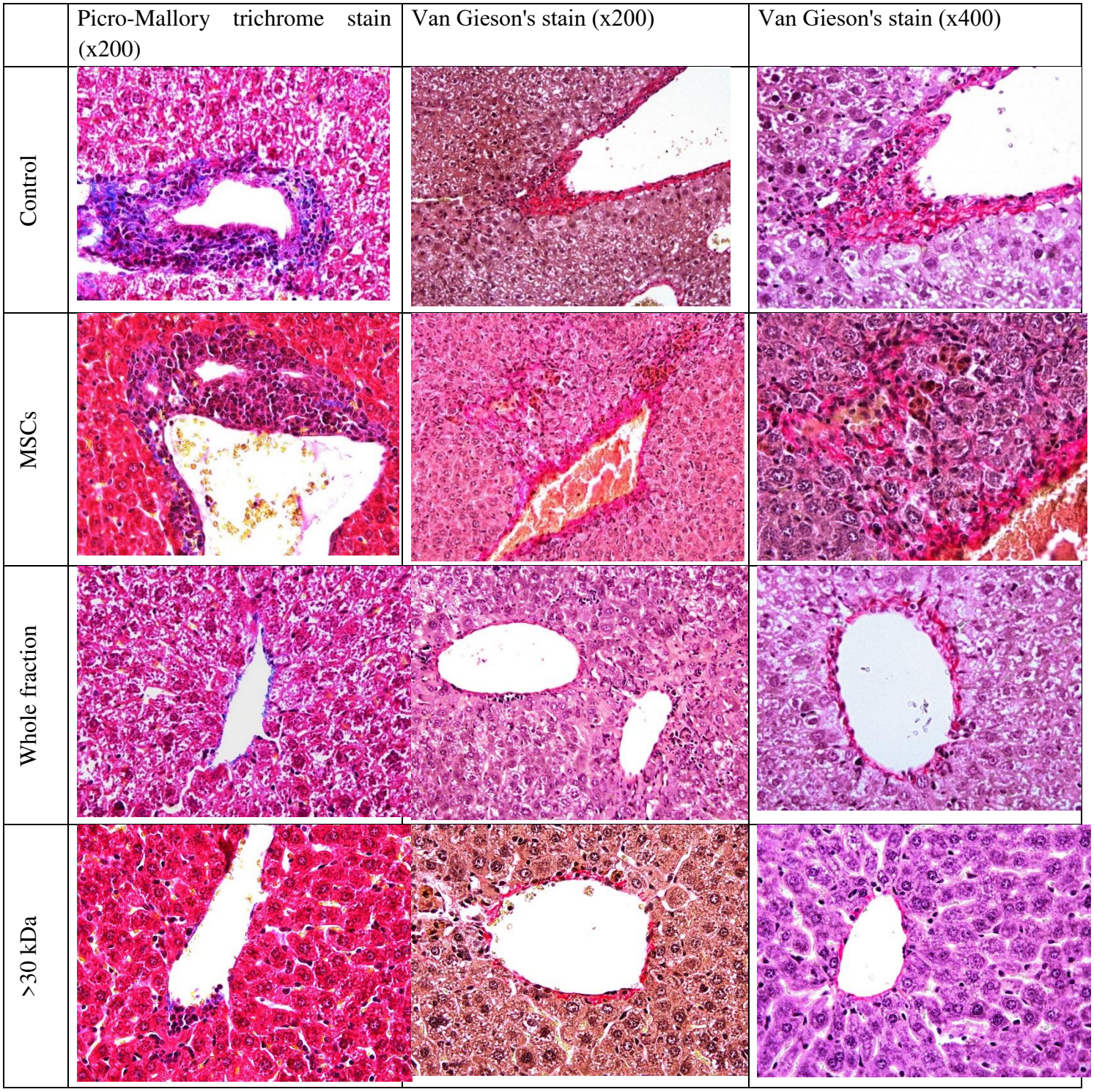

Figure 5. The impact of MSCs and CM on the growth of liver connective tissue in the presence of APAP

On day 10, during the fatty degeneration of hepatocytes and disruption of the plate structure of the lobules in the periportal region around the portal vein, a large number of collagen fibers (blue stain) preserving the cells of inflammatory infiltrate was observed in the control group (Fig. 5; Picro-Mallory staining, 200x magnification). Additional Van Gieson's staining also showed revealed disruption of the plate structure in the periportal region, and the adjacent hepatocytes were in a state of fatty degeneration. Inflammatory infiltration was preserved in the sclerotized periportal stroma (red stain; Van Gieson's stain, 200x magnification).

The disruption of the plate structure and the presence of an inflammatory infiltrate with a small amount of collagen fibers (weaker collagen formation compared to the control) were observed in the periportal zone of the hepatic lobule in the MSC group, as well as in the control. Degenerative changes in hepatocytes were not significant (Picro-Mallory trichrome stain, 200x magnification). Additional Van Gieson's staining revealed the site of sclerosis around the portal and central veins. Inflammatory infiltration persisted in the sclerotized areas (Van Gieson's stain, 200x magnification, 400x magnification).

Signs of minor sclerotic changes in the portal stroma containing single lymphocytes were noted under the effect of the whole fraction of CM (Van Gieson's stain, 200x magnification), as confirmed by Van Gieson's staining. It is important to note that the minimum growth of connective tissue was observed when using the conditioned medium and especially its 0-30 kDa fraction.

The effect of CM on the progression of aseptic inflammation.

The previous stage of the investigation testified that the >30 kDa fraction of the conditioned medium had the maximum anti-inflammatory activity, attended by the decrease in the level of granulocytic infiltration. Therefore, this fraction specifically was studied in the model of sterile inflammation.

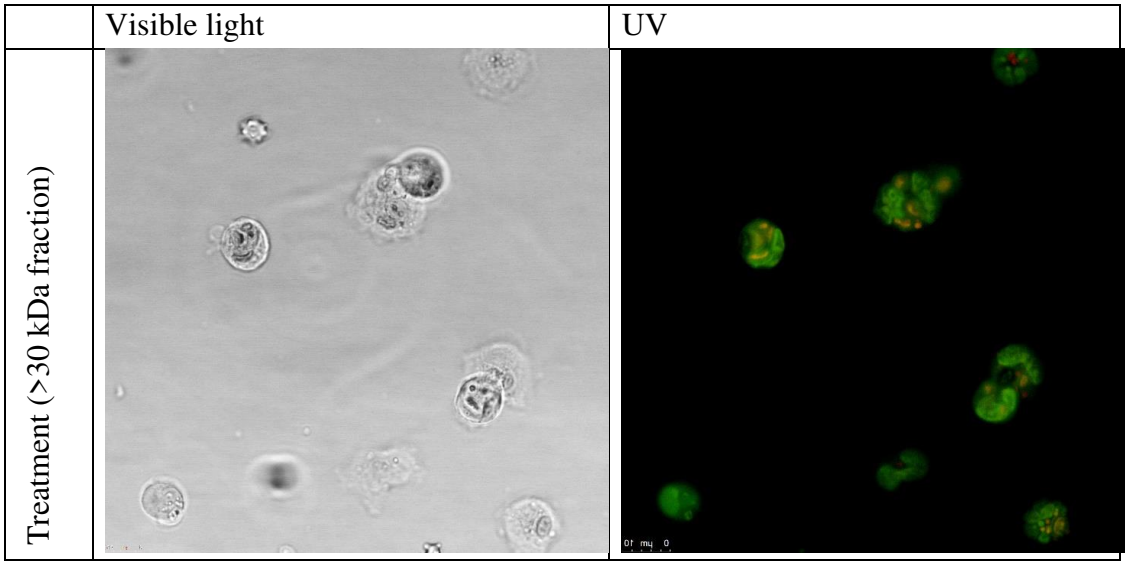

Figure 6. Cells of peritoneal exudate from animals in the control and treated groups (x400 magnification)

Staining with AO showed that, opposite to the control, neutrophils of peritoneal exudate obtained from animals simultaneously injected with zymosan and the >30 kDa fraction of CM contained granules in the cytoplasm that demonstrated a particular stain for single-stranded nucleic acids (Fig. 6). This fact may indicate an active phase of biosynthetic processes occurring in the cell.

Alternatively, Lundqvist-Gustafsson H and Bengtsson T showed that changes in the cells' morphological characteristics occur in neutrophils during early apoptosis induced by phorbol ester. The process is attended by the appearance of round or oval granules with fragments of dark purple nucleic chromatin in the cytoplasm [Lundqvist-Gustafsson H, Bengtsson T. 1999].

Therefore, the observed morphological changes in neutrophils occurring under the effect of the >30 kDa fraction of CM require further studying and could indicate either activation of protein synthesis in the cell or onset of apoptosis.

The hematological analysis of the blood of animals in the intact, control and treated groups revealed a change in the neutrophil-lymphocyte ratio (Table 4).

Table 4. The effect of >30 kDa fraction of CM on the neutrophil-lymphocyte ratio in the peripheral blood of animals in the treatment group/

	Neutrophil/lymphocyte ratio
Intact animal	2:1
Control animal	1:8
Treatment animal	1:1

As shown in Table 4, the neutrophil-lymphocyte ratio (NLR) in the blood of intact animals was 2/1 5 hours after the intraperitoneal injection of zymosan, decreasing to 1/8 in the control group. In the treated group, where animals were injected with the >30 kDa fraction of CM together with zymosan, NLR was 1/1. Thus, subcutaneous injection of the >30 kDa fraction of CM reduced the migration of neutrophils to the sites of inflammation and, obviously, inhibited the general inflammatory response in the animal body, as seen from the blood response to inflammation.

Chemiluminescence of neutrophils

One of the main functions of neutrophils is to produce ROS, thus, ensuring the antibacterial effect.

We discovered that in the peripheral blood of animals from the treated group, the integral index of ROS production significantly decreased in response to opsonized zymosan.

Our analysis demonstrated a significant decrease in the total ROS production and the amplitude of the chemiluminescent response the blood of animals in the treated group, as compared to the variables in the control group (Fig. 7)

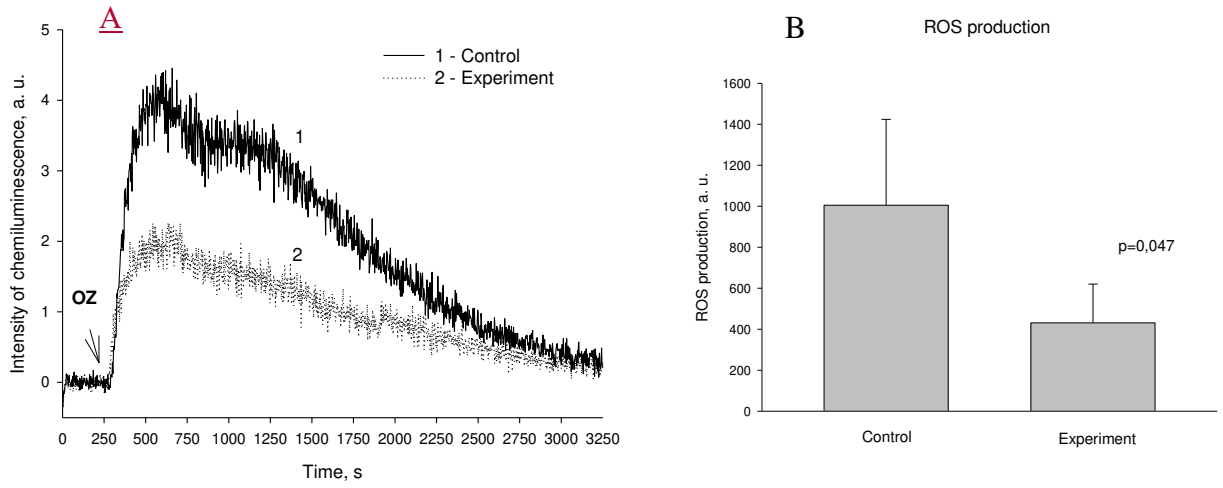

Figure 7. Generation of reactive oxygen species in the peripheral blood. A - experimental records of responses to opsonized zymosan in whole blood of control animals (1) and animals that received subcutaneous injection with the >30 kDa fraction of CM 4 h before assessment (2). B - change in total ROS production in response to opsonized zymosan in animals of the treated group.

ROS production (Fig. 7A) in neutrophils isolated from the inflammation site in the peritoneal cavity also varied across the studied groups of animals. The response to the bacterial peptide Nformyl-Met-Leu-Phe (fMLF), acting through receptors coupled to GTP-binding protein, was significantly lower in the cells of animals from the treated group than in the cells of the control group animals (Fig. 7A). The kinetic parameters of the response, such as the rate of the response development (slope) and the amplitude and ROS production, were significantly lower in the cells of the treated group animals compared to those of the control group (table 5). The obtained results suggest that the activity of NADPH oxidase, which catalyzes the development of superoxide anion radical (a precursor of other ROS), is changed in the cells of animals following an injection of the >30 kDa fraction of CM.

Table 5. Kinetic parameters of chemiluminescence normalized to control.

	Treatment (% to control)	p (to control)
Amplitude	49,4±24,2	0,000449
Total ROS production	50,7±23,7	0,000449
Angle of inclination	54,3±17,7	0,010734

The analysis of kinetic curves (Table 5) showed a significant difference between the production in the control and treated groups: total ROS production, the amplitude of the CL curve and tg of the angle of inclination of the curve, which characterizes the enzymatic activity of the NADPH complex.

Therefore, the >30 kDa fraction of CM altered the activity of intracellular enzymes (a decrease in the tg of the slope of the CL curve), leading to a significant reduction in the total production of ROS by neutrophils, both in the peripheral blood and at the inflammation site.

DISCUSSION

The conditioned medium derived through cultivation of mesenchymal stem cells reduces the extent of liver tissue damage caused by APAP. The analysis of the liver tissue of animals from the treated groups showed a lowered intensity of granulocytic infiltration, which, in our opinion, directly correlates with the expansion of liver parenchyma necrosis (as evidenced by the level of cytolytic enzyme). In the long term, this effect could develop by decreasing the severity of fibrous tissue formation. Possible reasons underlying this process include suppression of fibroblast proliferation caused by CM peptides or decreased initial inflammatory damage to the parenchyma.

The effect of CM on the functional activity of neutrophils requires particular attention. When using a classic activation agent, such as opsonized zymosan or fMLP, the signal from the receptor is transmitted to protein kinase C (PKC), activating NADPH oxidase and forming O_2^- radical. A possible reason for the decrease in ROS production in the blood and inflammatory sites can be a change in the NADPH oxidase activity, as well as in the activity of PKC, which facilitates phosphorylation of this oxidase complex. Studies of B. Saberi et al. have shown that with the effect of APAP, PKC becomes involved in hepatotoxicity, and the use of PKC inhibitors effectively (up to 80%) reduces the extent of ROS-mediated necrosis in hepatocytes (Saberi B et al. 2008; Saberi B et al. 2014). Alternatively, NADPH oxidase, which is involved in ROS production, is activated in hepatocytes by APAP, and inhibition of this complex reduces the severity of damage. In our study, MPO inhibition made it possible to isolate NADPH oxidase from the CL response, and its 45% reduction in granulocytes might be a potential cause of the decrease in the severity of liver damage.

It is important to mention that the liver damage stage is associated with neutrophil migration into the sterile inflammation region. This process is activated by the cell decay products that enter the bloodstream and cause the development of a systemic inflammatory reaction. Currently, there is no certain answer to the question of whether neutrophils are or are not involved into the process of further liver tissue injury. On the one hand, APAP is a chemical interceptor of free oxygen radicals and one could question the argument that there are no products of free-radical reaction in liver tissues (Freitas M et al. 2013). On the other hand, one of the main functions of neutrophils is the enzymatic destruction of dead or dying cell structures. Therefore, after active migration into the cell of a tissue containing a large number of hydrolytic enzymes in the cytoplasm, these enzymes are likely to be released, increasing the damage (Wright DI 1982). It is also worth noting that there is no data in the available literature that would suggest that neutrophils migrate from the liver to other organs and tissues after the completion of an active phase of inflammation. Thus, the further fate of neutrophils, and, most importantly, their death, remains unknown.

The stage of parenchyma damage is followed by the regeneration of hepatocytes and restoration of the liver architecture. Normally, after a single toxic impact of APAP, the liver

becomes completely restored. However, there are several studies that show that APAP can trigger the connective tissue formation both in the liver and in other organs, a fact which can be accounted as a consequence of massive hepatocyte death (Bai Q et al. 2017; AlWahsh M et al. 2019; Yu YL et al. 2014).

Hereby the investigated CM product (especially its >30 kDa fraction) influences both the stage of the acute liver injury and the stage of regeneration. This study, as well as our previous research, testified almost no hepatocyte death after the administration of the >30 kDa CM fraction under the toxic effect of APAP, compared to the control (Temnov AA et al 2019; Temnov A et al. 2019).

The reason for this effect may be a decrease in the protein synthetic or proliferative activity of hepatocytes. Similarly to the cytotoxic effect of ionizing radiation, which is most dangerous for rapidly dividing cells, CM peptides that suppress Ki-67 expression can make hepatocytes immune to the toxin, and the stimulation of proliferation that occurs upon MSC transplantation leads to an abruptly intensified cell death, exceeding the reference control values.

Another reason for the decrease in damage during the first stage may be an increase in the activity of endogenous antioxidants such as thioredoxin, which is increased in expression under the effect of CM (Lee BW et al. 2018) and can protect the liver from toxic effects by inactivation of reactive oxygen species. The impact of CM during the second stage is associated with inhibition of neutrophil migration to the liver, which could be the main reason for the reduced damage.

Using the model of sterile inflammation produced by administration of zymosan, our study showed that conditioned medium (>30 kDa fraction) has a systemic anti-inflammatory effect, which may be associated with a disruption in the granulocyte migration to the inflammation site and a decrease in ROS production. Decreased number of neutrophils at the site of sterile inflammation and weak inflammatory reaction of blood compared to the control, demonstrated under the administration of CM, may be associated with inhibition of proliferation, which occurs in the liver tissue (compared to the control), and possibly appears at the systemic level. It remains unclear whether CM has a direct inhibitory effect on fibroblasts in the liver; this topic requires further study.

Acknowledgments

This study was supported by the Russian Foundation for Basic Research (grant no. 18-29-17059).

The authors are grateful to A.D. Kobzev (Secondary School No. 1212) for participation in the evaluation of scientific evidence.

Compliance with ethical standards

Conflict of interest The authors declare that they have no conflict of interest.

Research involving animals The study protocol was approved by the institutional Ethics Committee of the Institute of Cell Biophysics RAS (PSCBR RAS) and were in compliance with ARRIVE guidelines. All methods were also performed in accordance with the relevant guidelines and regulations. All the experiments were carried out according to international

regulations listed in the European Convention for the Protection of Vertebrate Animals used for Experimental and Other Scientific Purposes (ETS 123) and ICB RAS. Manual for Working with Laboratory Animal no. 57 (30.12.2011).

Informed consent Informed consent was obtained from all individual participants included in the study.

REFERENCES

AlWahsh M, Othman A, Hamadneh L, Telfah A, Lambert J, Hikmat S, Alassi A, Mohamed FEZ, Hergenröder R, Al-Qirim T, Dooley S, Hammad S. Second exposure to acetaminophen overdose is associated with liver fibrosis in mice. EXCLI J. 2019 Feb 6;18:51-62. PMID: 30956639; PMCID: PMC6449668.

Bai Q, Yan H, Sheng Y, Jin Y, Shi L, Ji L, Wang Z. Long-term acetaminophen treatment induced liver fibrosis in mice and the involvement of Egr-1. Toxicology. 2017 May 1;382:47-58. doi: 10.1016/j.tox.2017.03.008. Epub 2017 Mar 9. PMID: 28286204.

Cover C, Liu J, Farhood A, Malle E, Waalkes MP, Bajt ML, Jaeschke H. Pathophysiological role of the acute inflammatory response during acetaminophen hepatotoxicity. Toxicol Appl Pharmacol. 2006 Oct 1;216(1):98-107. doi: 10.1016/j.taap.2006.04.010. Epub 2006 Jun 16. PMID: 16781746;

Foyouzi-Youssefi R, Petersson F, Lew DP, Krause KH, Nüsse O. Chemoattractant-induced respiratory burst: increases in cytosolic Ca2+ concentrations are essential and synergize with a kinetically distinct second signal. Biochem J. 1997 Mar 15;322 (Pt 3)(Pt 3):709-18. doi: 10.1042/bj3220709. PMID: 9148740; PMCID: PMC1218246.

Freitas M, Costa VM, Ribeiro D, Couto D, Porto G, Carvalho F, Fernandes E. Acetaminophen prevents oxidative burst and delays apoptosis in human neutrophils. Toxicol Lett. 2013 May 23;219(2):170-7. doi: 10.1016/j.toxlet.2013.03.007. Epub 2013 Mar 18. PMID: 23518321.

Hou HS, Liao CL, Sytwu HK, Liao NS, Huang TY, Hsieh TY, Chu HC. Deficiency of interleukin-15 enhances susceptibility to acetaminophen-induced liver injury in mice. PLoS One. 2012;7(9):e44880. doi: 10.1371/journal.pone.0044880. Epub 2012 Sep 18. PMID: 23028657; PMCID: PMC3445599.

Ishida Y, Kondo T, Kimura A, Tsuneyama K, Takayasu T, Mukaida N. Opposite roles of neutrophils and macrophages in the pathogenesis of acetaminophen-induced acute liver injury. Eur J Immunol. 2006 Apr;36(4):1028-38. doi: 10.1002/eji.200535261. PMID: 16552707.

Jaeschke H, Williams CD, Ramachandran A, Bajt ML. Acetaminophen hepatotoxicity and repair: the role of sterile inflammation and innate immunity. Liver Int. 2012 Jan;32(1):8-20. doi: 10.1111/j.1478-3231.2011.02501.x. Epub 2011 Mar 14. PMID: 21745276; PMCID: PMC3586825.

Larson AM. Acetaminophen hepatotoxicity. Clin Liver Dis. 2007 Aug;11(3):525-48, vi. doi: 10.1016/j.cld.2007.06.006. PMID: 17723918.

Lawson JA, Farhood A, Hopper RD, Bajt ML, Jaeschke H. The hepatic inflammatory response after acetaminophen overdose: role of neutrophils. Toxicol Sci. 2000 Apr;54(2):509-16. doi: 10.1093/toxsci/54.2.509. PMID: 10774834.

Lee BW, Jeon BS, Yoon BI. Exogenous recombinant human thioredoxin-1 prevents acetaminophen-induced liver injury by scavenging oxidative stressors, restoring the thioredoxin-1 system and inhibiting receptor interacting protein-3 overexpression. J Appl Toxicol. 2018 Jul;38(7):1008-1017. doi: 10.1002/jat.3609. Epub 2018 Mar 7. PMID: 29512171.

Liu ZX, Han D, Gunawan B, Kaplowitz N. Neutrophil depletion protects against murine acetaminophen hepatotoxicity. Hepatology. 2006 Jun;43(6):1220-30. doi: 10.1002/hep.21175. PMID: 16729305.

Lundqvist-Gustafsson H, Bengtsson T. Activation of the granule pool of the NADPH oxidase accelerates apoptosis in human neutrophils. J Leukoc Biol. 1999 Feb;65(2):196-204. doi: 10.1002/jlb.65.2.196. PMID: 10088602.

Marques PE, Amaral SS, Pires DA, Nogueira LL, Soriani FM, Lima BH, Lopes GA, Russo RC, Avila TV, Melgaço JG, Oliveira AG, Pinto MA, Lima CX, De Paula AM, Cara DC, Leite MF, Teixeira MM, Menezes GB. Chemokines and mitochondrial products activate neutrophils to amplify organ injury during mouse acute liver failure. Hepatology. 2012 Nov;56(5):1971-82. doi: 10.1002/hep.25801. Epub 2012 Aug 21. PMID: 22532075.

McGill MR, Jaeschke H. Metabolism and disposition of acetaminophen: recent advances in relation to hepatotoxicity and diagnosis. Pharm Res. 2013 Sep;30(9):2174-87. doi: 10.1007/s11095-013-1007-6. Epub 2013 Mar 6. PMID: 23462933; PMCID: PMC3709007.

McGill MR, Sharpe MR, Williams CD, Taha M, Curry SC, Jaeschke H. The mechanism underlying acetaminophen-induced hepatotoxicity in humans and mice involves mitochondrial damage and nuclear DNA fragmentation. J Clin Invest. 2012 Apr;122(4):1574-83. doi: 10.1172/JCI59755. Epub 2012 Mar 1. PMID: 22378043; PMCID: PMC3314460.

Saberi B, Shinohara M, Ybanez MD, Hanawa N, Gaarde WA, Kaplowitz N, Han D. Regulation of H(2)O(2)-induced necrosis by PKC and AMP-activated kinase signaling in primary cultured hepatocytes. Am J Physiol Cell Physiol. 2008 Jul;295(1):C50-63. doi: 10.1152/ajpcell.90654.2007. Epub 2008 May 7. PMID: 18463227; PMCID: PMC2493548.

Saberi B, Ybanez MD, Johnson HS, Gaarde WA, Han D, Kaplowitz N. Protein kinase C (PKC) participates in acetaminophen hepatotoxicity through c-jun-N-terminal kinase (JNK)-dependent and -independent signaling pathways. Hepatology. 2014 Apr;59(4):1543-1554. doi: 10.1002/hep.26625. Epub 2014 Mar 3. PMID: 23873604; PMCID: PMC3997165.

Schmittgen TD, Livak KJ. Analyzing real-time PCR data by the comparative C(T) method. Nat Protoc. 2008;3(6):1101-8. doi: 10.1038/nprot.2008.73. PMID: 18546601.

Temnov A, Rogov K, Zhalimov V, Igor P, Pekov S, Bader A, Sklifas A, Giri S. The effect of a mesenchymal stem cell conditioned medium fraction on morphological characteristics of hepatocytes in acetaminophen-induced acute liver failure: a preliminary study. Hepat Med.

2019 Jul 19;11:89-96. doi: 10.2147/HMER.S196354. PMID: 31410073; PMCID: PMC6650605.

Temnov AA, Rogov KA, Sklifas AN, Klychnikova EV, Hartl M, Djinovic-Carugo K, Charnagalov A. Protective properties of the cultured stem cell proteome studied in an animal model of acetaminophen-induced acute liver failure. Mol Biol Rep. 2019 Jun;46(3):3101-3112. doi: 10.1007/s11033-019-04765-z. Epub 2019 Apr 12. PMID: 30977085.

Tikhonova IV, Kosyakova NI, Grinevich AA, Nadeev AD, Chemeris NK, Safronova VG. Accelerated reactivity of blood granulocytes in patients with atopic bronchial asthma out of exacerbation. Immunobiology. 2018 Jan;223(1):8-17. doi: 10.1016/j.imbio.2017.10.020. Epub 2017 Oct 5. PMID: 29032837.

Wang JX, Zhang C, Fu L, Zhang DG, Wang BW, Zhang ZH, Chen YH, Lu Y, Chen X, Xu DX. Protective effect of rosiglitazone against acetaminophen-induced acute liver injury is associated with down-regulation of hepatic NADPH oxidases. Toxicol Lett. 2017 Jan 4;265:38-46. doi: 10.1016/j.toxlet.2016.11.012. Epub 2016 Nov 17. PMID: 27866976.

Williams CD, Bajt ML, Farhood A, Jaeschke H. Acetaminophen-induced hepatic neutrophil accumulation and inflammatory liver injury in CD18-deficient mice. Liver Int. 2010 Oct;30(9):1280-92. doi: 10.1111/j.1478-3231.2010.02284.x. PMID: 20500806; PMCID: PMC4278356.

Williams CD, Bajt ML, Sharpe MR, McGill MR, Farhood A, Jaeschke H. Neutrophil activation during acetaminophen hepatotoxicity and repair in mice and humans. Toxicol Appl Pharmacol. 2014 Mar 1;275(2):122-33. doi: 10.1016/j.taap.2014.01.004. Epub 2014 Jan 15. PMID: 24440789; PMCID: PMC3941640.

Williams CD, Farhood A, Jaeschke H. Role of caspase-1 and interleukin-1beta in acetaminophen-induced hepatic inflammation and liver injury. Toxicol Appl Pharmacol. 2010 Sep 15;247(3):169-78. doi: 10.1016/j.taap.2010.07.004. Epub 2010 Jul 15. PMID: 20637792; PMCID: PMC2929281.

Wright DI The neutrophils as a secretory organ of host defense// Advances in host defense mechanisms. N.Y. , 1982. Vol.1, p75-110

Yagi H, Soto-Gutierrez A, Navarro-Alvarez N, Nahmias Y, Goldwasser Y, Kitagawa Y, Tilles AW, Tompkins RG, Parekkadan B, Yarmush ML. Reactive bone marrow stromal cells attenuate systemic inflammation via sTNFR1. Mol Ther. 2010 Oct;18(10):1857-64. doi: 10.1038/mt.2010.155. Epub 2010 Jul 27. PMID: 20664529; PMCID: PMC2951565.

Yu YL, Yiang GT, Chou PL, Tseng HH, Wu TK, Hung YT, Lin PS, Lin SY, Liu HC, Chang WJ, Wei CW. Dual role of acetaminophen in promoting hepatoma cell apoptosis and kidney fibroblast proliferation. Mol Med Rep. 2014 Jun;9(6):2077-84. doi: 10.3892/mmr.2014.2085. Epub 2014 Mar 28. PMID: 24682227; PMCID: PMC4055434.

Figures

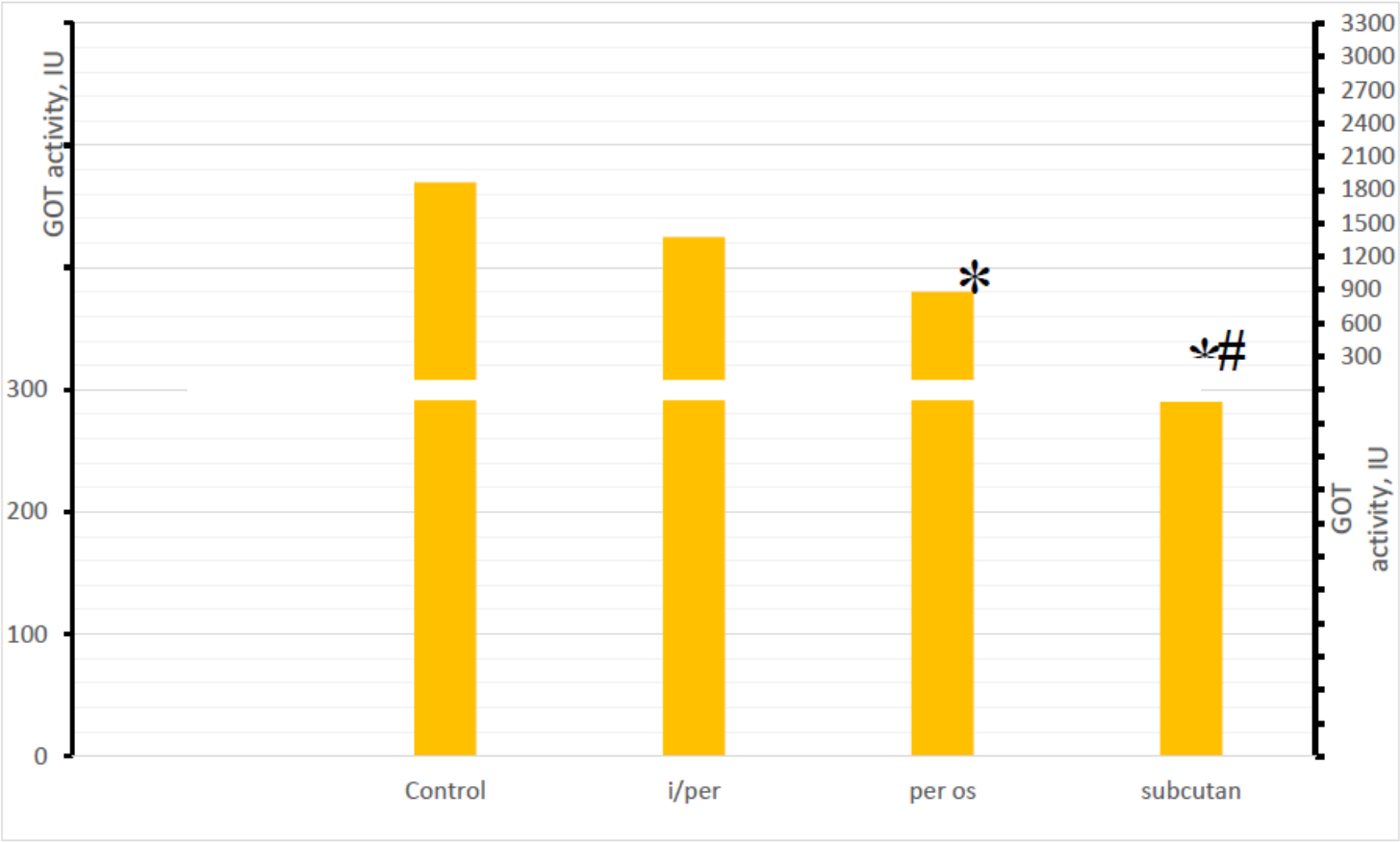

Figure 1

Activities of liver enzyme GOT (n=15 for each group) in the control group and in animals treated with CM hours after administration of APAP. *- true for the control group ($p<0.05$); #- true for other groups ($p<0.05$).

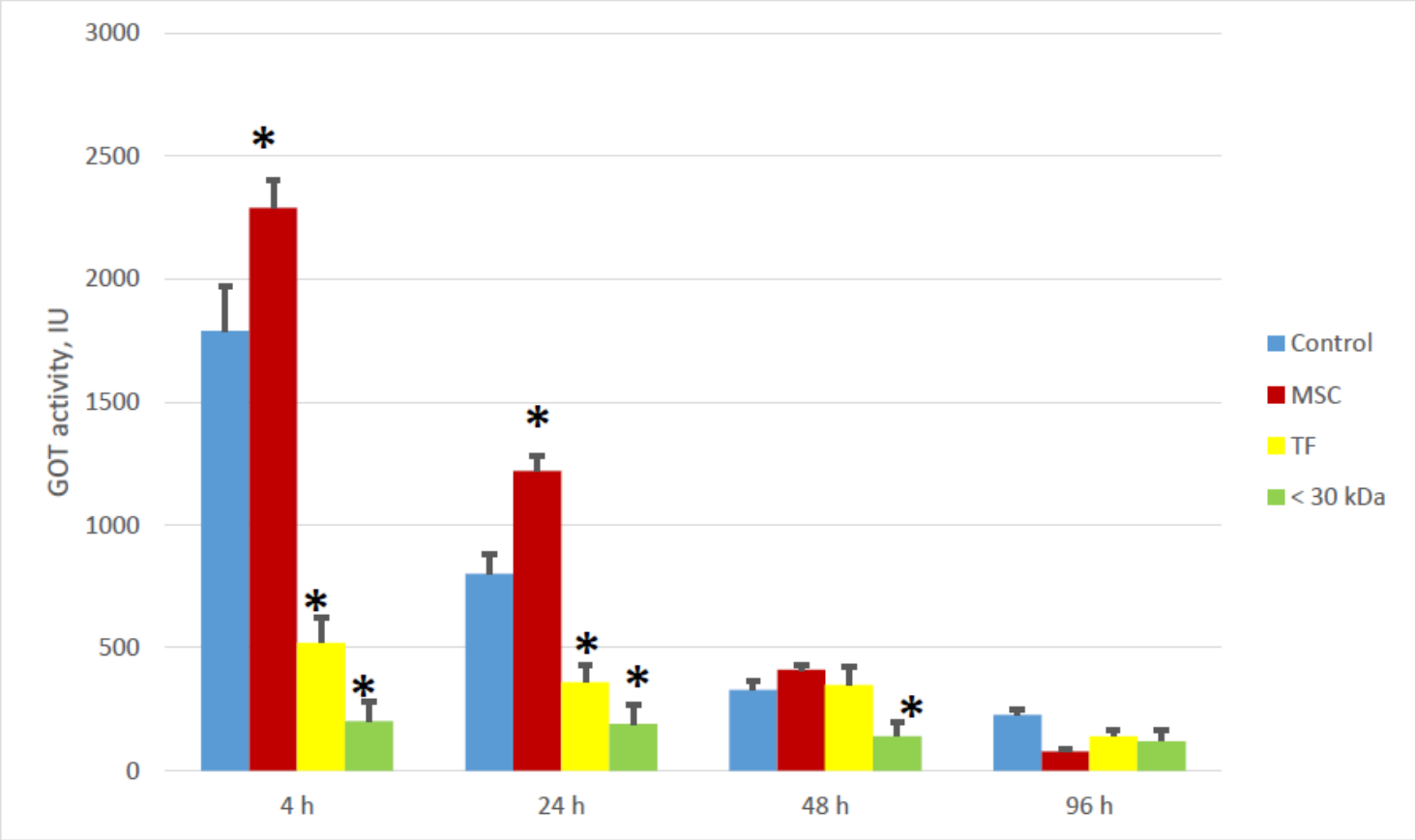

Figure 2

Changes in the activity of GOT under the influence of MSCs and CM in the blood under administration of APAP. *- true for the control group ($p<0.05$).

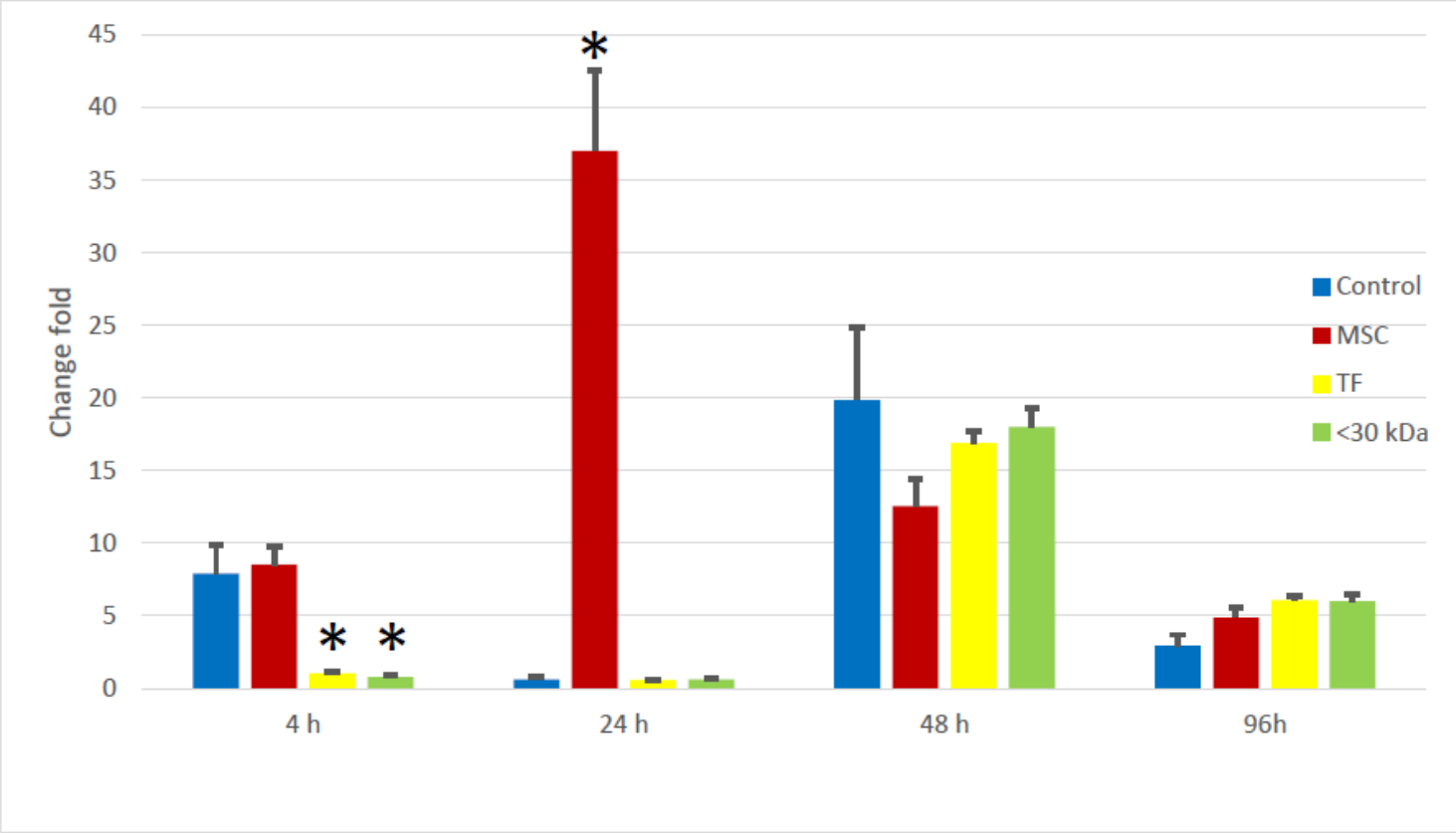

Figure 3

Changes in the expression of the Ki-67 gene (mRNA level) under the influence of MSCs and CM in the liver tissue. Data normalized to beta-actin . *- true for the control group ($p<0.05$).

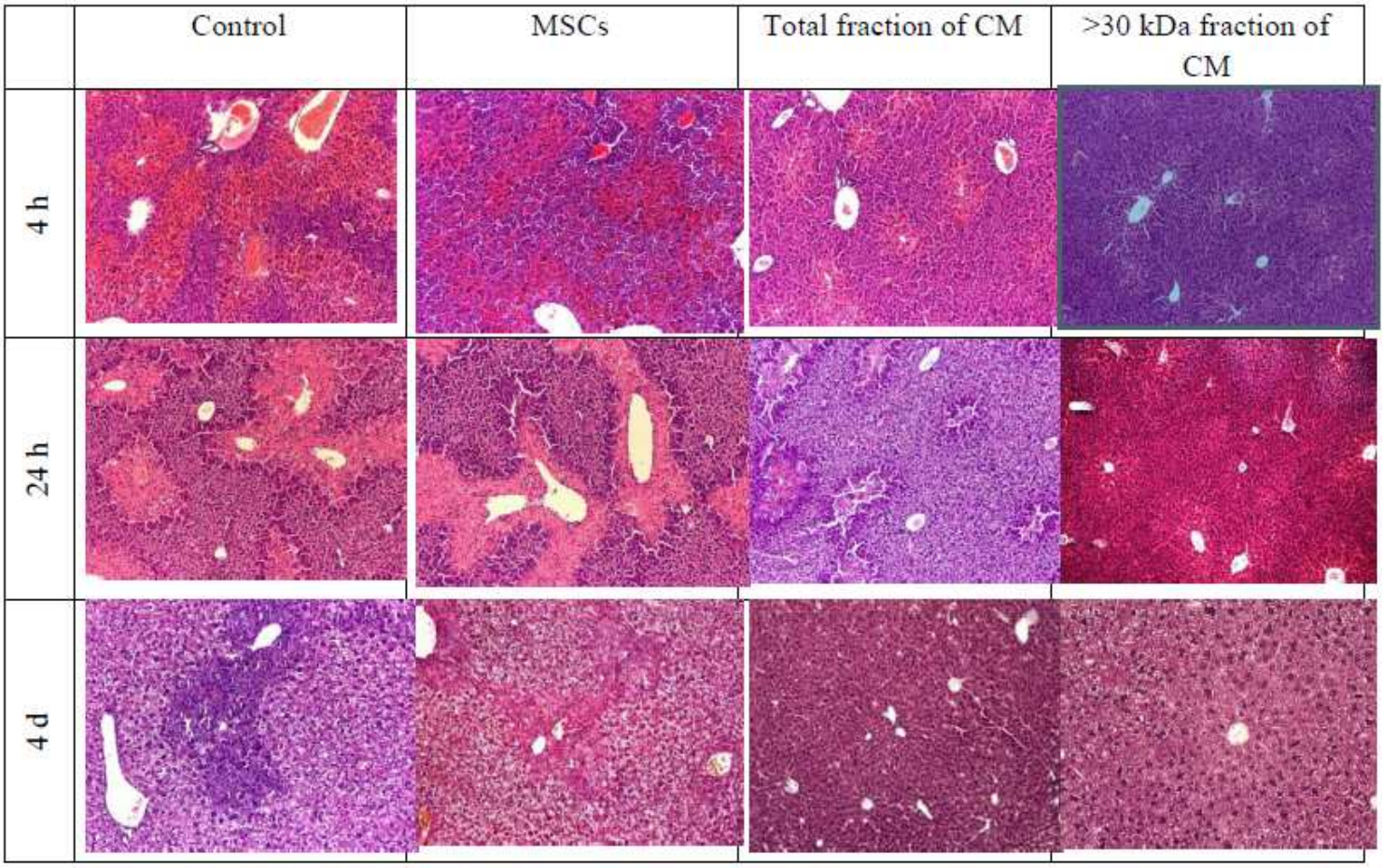

Figure 4

The effect of MSCs and CM on liver histology in the presence of APAP

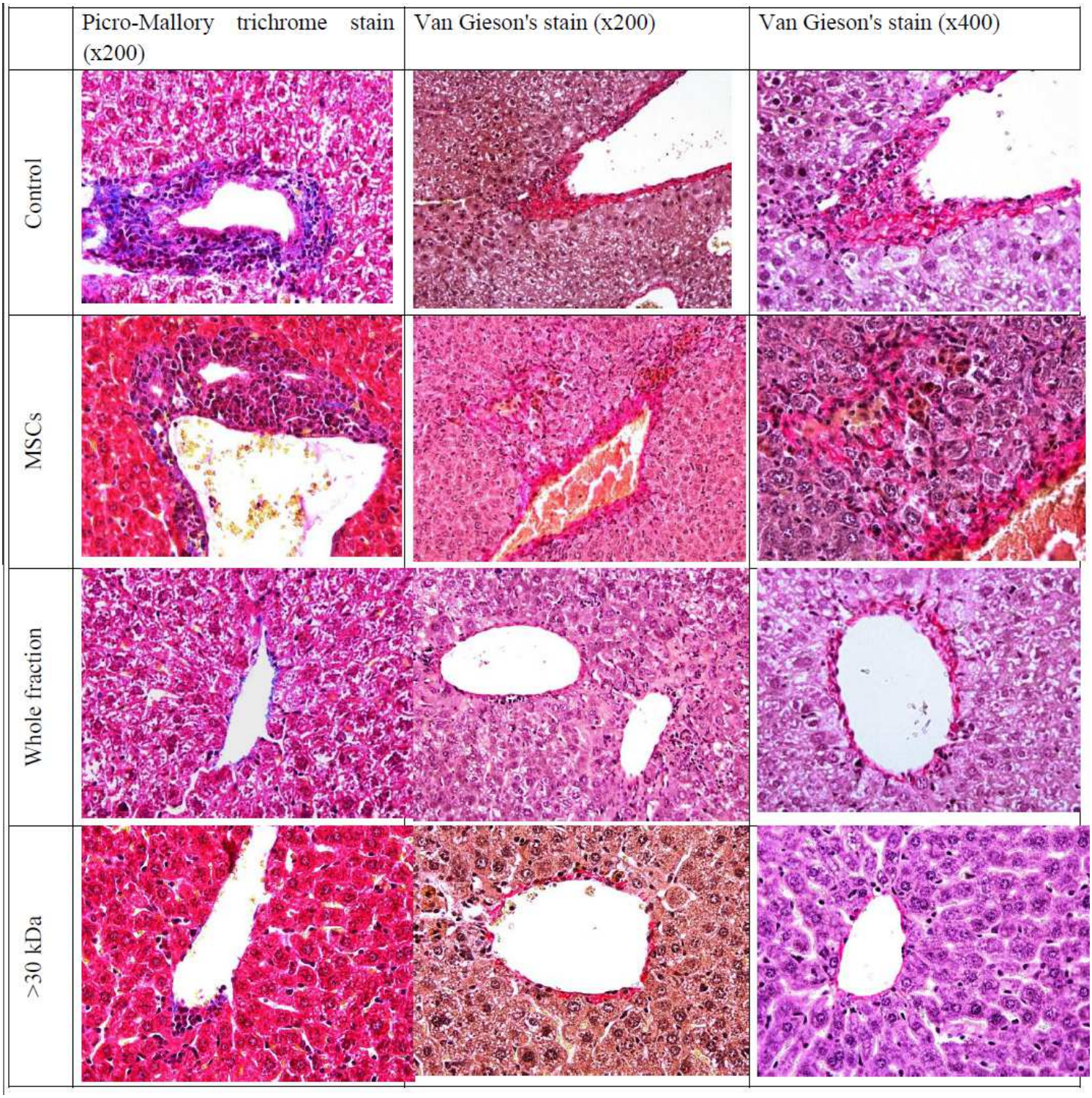

Figure 5

The impact of MSCs and CM on the growth of liver connective tissue in the presence of APAP

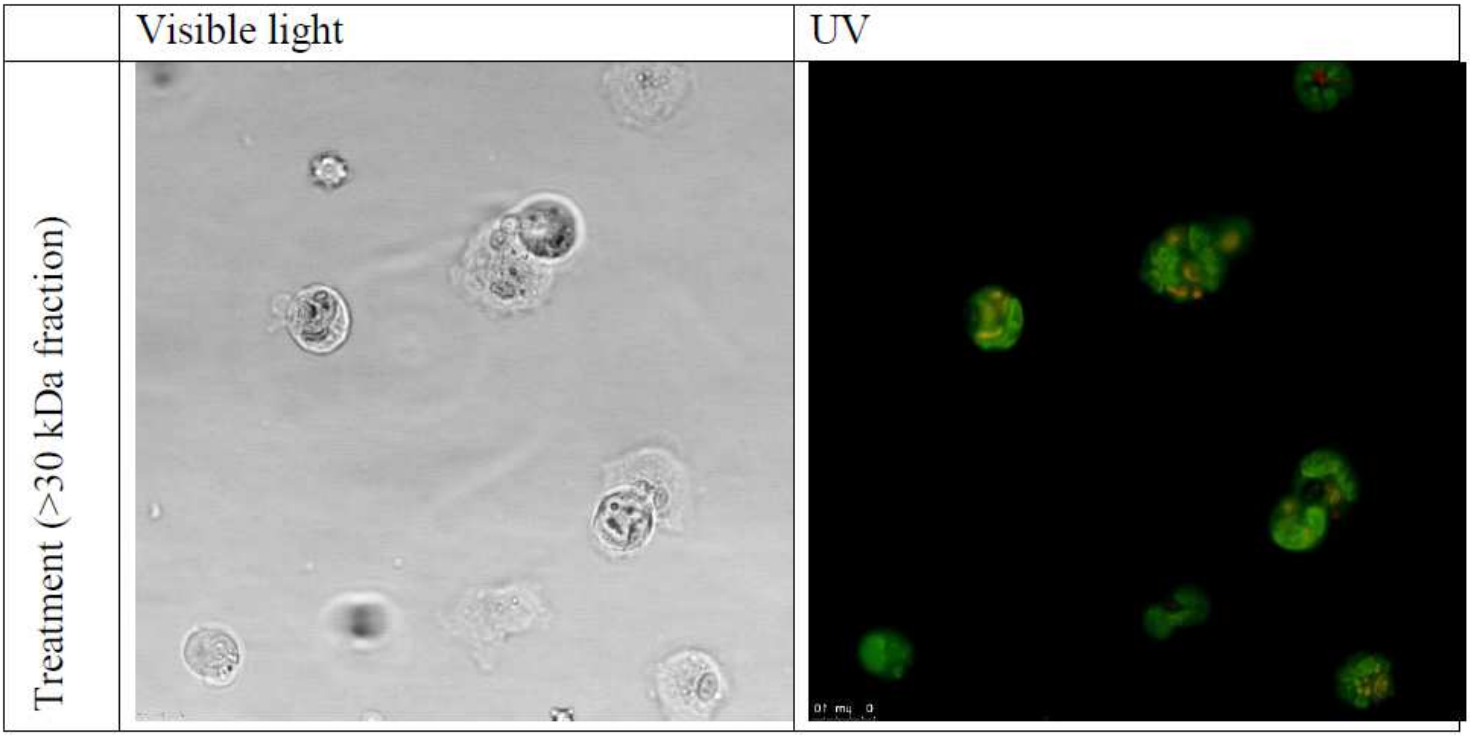

Figure 6

Cells of peritoneal exudate from animals in the control and treated groups (x400 magnification)

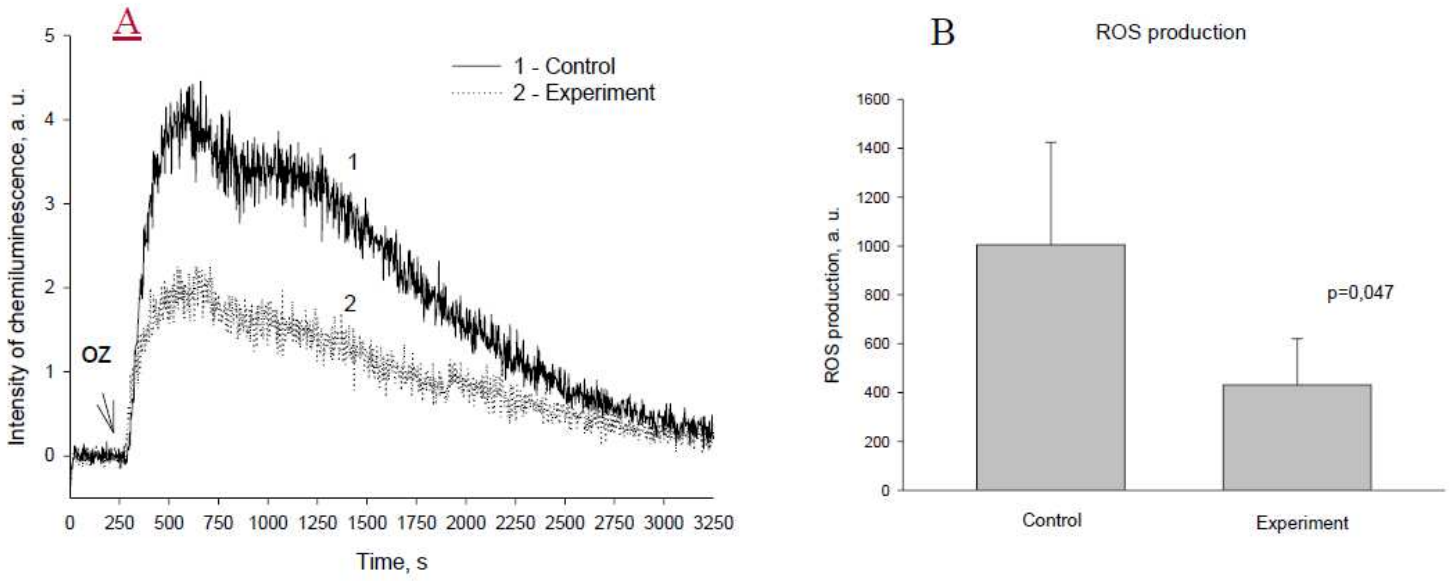

Figure 7

Generation of reactive oxygen species in the peripheral blood. A - experimental records of responses to opsonized zymosan in whole blood of control animals (1) and animals that received subcutaneous injection with the >30 kDa fraction of CM 4 h before assessment (2). B - change in total ROS production in response to opsonized zymosan in animals of the treated group.